

# Pairing strengths for a two orbital model of the Fe-pnictides

Xiao-Liang Qi<sup>1</sup>, S. Raghu<sup>1</sup>, Chao-Xing Liu<sup>2,1</sup>, D. J. Scalapino<sup>3</sup> and Shou-Cheng Zhang<sup>1</sup>

<sup>1</sup>*Department of Physics, McCullough Building, Stanford University, Stanford, CA 94305-4045*

<sup>2</sup>*Center for Advanced Study, Tsinghua University, Beijing, 100084, R. P. China and*

<sup>3</sup>*Department of Physics, University of California, Santa Barbara, CA 93106-9530*

(Dated: August 16, 2021)

Using an RPA approximation, we have calculated the strengths of the singlet and triplet pairing interactions which arise from the exchange of spin and orbital fluctuations for a 2-orbital model of the Fe-pnictide superconductors. When the system is doped with F, the electron pockets become dominant and we find that the strongest pairing occurs in the singlet d-wave pairing and the triplet p-wave pairing channels, which compete closely. The pairing structure in the singlet d-wave channel corresponds to a superposition of near neighbor intra-orbital singlets with a minus sign phase difference between the  $d_{xz}$  and  $d_{yz}$  pairs. The leading pairing configuration in the triplet channel also involves a nearest neighbor intra-orbital pairing. We find that the strengths of both the singlet and triplet pairing grow, with the singlet pairing growing faster, as the onsite Coulomb interaction approaches the value where the  $S = 1$  particle-hole susceptibility diverges.

PACS numbers: 71.10.Fd, 71.18.+y, 71.20.-b, 74.20.-z, 74.20.Mn, 74.25.Ha, 75.30.Fv

Recently, a new class of superconductors involving a family of Fe-based oxypnictides has been discovered[1, 2, 3, 4, 5, 6, 7, 8, 9]. With  $T_c$  as high as 55K[7], the mechanism of superconductivity is likely to be electronic in origin and consequently, these materials have generated tremendous excitement. Moreover, experimental results including specific heat[10, 11], point-contact spectroscopy[12], high-field resistivity[13, 14] and NMR [15] measurements suggest the existence of unconventional superconductivity in these materials. Furthermore, transport[16] and neutron scattering[17] measurements in LaOFeAs have shown the evidence of spin-density-wave (SDW) magnetic order below  $T = 137K$ . An experimental determination of the orbital and spin state of the Cooper pairs, however, has not yet been made.

Band structure calculations show that the Fermi surface of F doped LaOFeAs consists of two nearly concentric hole cylinders surrounding the  $\Gamma$  point and two elliptically distorted electron cylinders around the M point of the 2Fe/cell Brillouin zone. Electronic transitions involving states on one or between two of these Fermi surface sheets lead to q-dependent structure in the spin and orbital susceptibilities. For small doping, the electron and the hole fermi surfaces are of comparable sizes, and their nesting can give rise to the observed SDW order in the undoped material [16, 17]. Upon further doping, the two hole pockets shrink, the electron fermi surfaces become dominant [18], and the system exhibits superconductivity. Ref. [19] suggests that a triplet p-wave pairing state is obtained on the electron Fermi surfaces due to the ferromagnetic spin fluctuations. Other related possibilities have also been discussed in the literature, including inter-orbital on-site triplet pairing [20, 21], and a s-wave pairing state which changes sign from the electron to the hole pockets [22].

Recently, we have introduced a tight-binding model

[23] with “ $d_{xz}$ ” and “ $d_{yz}$ ” orbitals on a two-dimensional square lattice of “Fe” sites. This simple tight-binding model correctly reproduces the topology of both the electron and the hole fermi surfaces. It also reproduces the van Hove singularities obtained in bandstructure calculations. For low doping, when the electron and hole pockets are comparable, RPA calculations show enhanced SDW fluctuations at the wave vectors  $(\pi, 0)$  and  $(0, \pi)$ , defined in the convention of one Fe atom per unit cell [23]. In this work we investigate the nature of the pairing state when this model is further doped. With on-site inter-orbital and intra-orbital Coulomb interaction terms, we use the RPA approximation to study the effective pair interaction vertex induced by the spin and orbital fluctuations. We find that when the doping is increased and the electron pockets become larger, the leading pairing instability occurs in the singlet d-wave and the triplet p-wave channels. The pairing strength for both channels increases as the system approaches an instability in the  $S = 1$  particle-hole channel, with the singlet d-wave channel growing faster than the triplet p-wave channel.

*Model Hamiltonian* - Our tight-binding model Hamiltonian describes a square two-dimensional “Fe” lattice with two orbitals per site

$$H_0 = \sum_{k\sigma} \psi_{k\sigma}^\dagger [(\epsilon_+(k) - \mu) 1 + \epsilon_-(k)\tau_3 + \epsilon_{xy}(k)\tau_1] \psi_{k\sigma} \quad (1)$$

Here  $\sigma$  is the spin index,  $\tau_i$  are Pauli matrices and  $\psi_{k\sigma}^\dagger = [d_{x\sigma}^\dagger(k), d_{y\sigma}^\dagger(k)]$  is a two-component field, which describes the two degenerate “ $d_{xz}$ ” and “ $d_{yz}$ ” orbitals. The matrix elements of  $H_0$ ,  $\epsilon_+(\mathbf{k}) = -(t_1 + t_2)(\cos k_x + \cos k_y) - 4t_3 \cos k_x \cos k_y$ ,  $\epsilon_-(\mathbf{k}) = -(t_1 - t_2)(\cos k_x - \cos k_y)$  and  $\epsilon_{xy}(\mathbf{k}) = -4t_4 \sin k_x \sin k_y$  are parametrized by four hopping parameters  $t_i, i = 1, \dots, 4$ .

This free fermion Hamiltonian is diagonalized by introducing a canonical transformation to the band operators

$\gamma_{\nu\sigma,\mathbf{k}}$ :

$$\psi_{s\sigma,\mathbf{k}} = \sum_{\nu=\pm} a_{\nu,\mathbf{k}}^s \gamma_{\nu\sigma,\mathbf{k}} \quad (2)$$

with

$$\begin{aligned} a_{\nu,\mathbf{k}}^s &= \langle s | \nu, \mathbf{k} \rangle \\ a_{+,\mathbf{k}}^x &= a_{-,\mathbf{k}}^y = \text{sgn}(\epsilon_{xy}(\mathbf{k})) \sqrt{\frac{1}{2} + \frac{\epsilon_{-}(\mathbf{k})}{2\sqrt{\epsilon_{-}^2(\mathbf{k}) + \epsilon_{xy}^2(\mathbf{k})}}} \\ a_{+,\mathbf{k}}^y &= -a_{-,\mathbf{k}}^x = \sqrt{\frac{1}{2} - \frac{\epsilon_{-}(\mathbf{k})}{2\sqrt{\epsilon_{-}^2(\mathbf{k}) + \epsilon_{xy}^2(\mathbf{k})}}} \end{aligned} \quad (3)$$

the wave-function of the  $\nu$  band with  $\nu = \pm 1$ , and  $\gamma_{\nu\sigma,\mathbf{k}}$  the annihilation operator of an electron with spin  $\sigma$  and wave-vector  $\mathbf{k}$  in the  $\nu$  band. With the inclusion of a chemical potential  $\mu$ , the band part of the Hamiltonian becomes

$$H_0 = \sum_{\mathbf{k}\sigma\nu} (E_{\nu}(\mathbf{k}) - \mu) \gamma_{\nu\sigma,\mathbf{k}}^{\dagger} \gamma_{\nu\sigma,\mathbf{k}}, \quad \nu = \pm \quad (4)$$

with  $E_{\pm}(\mathbf{k}) = \epsilon_{+}(\mathbf{k}) \pm \sqrt{\epsilon_{-}^2(\mathbf{k}) + \epsilon_{xy}^2(\mathbf{k})}$ . The tight binding parameters  $t_i$  can be adjusted to fit the Fermi surface obtained from LDA band structure calculations [19, 22, 24]. In this work, we will take the parameters  $t_1 = -1, t_2 = 1.3, t_3 = t_4 = -0.85$  and measure energy in units of  $|t_1|$ . With a chemical potential  $\mu = 1.45$ , one has a filling of 2 electrons per site, a Fermi surface similar to bandstructure calculation of lightly doped LaOFeAs and a peak in the bare spin susceptibility for  $q = (\pi, 0)$  and  $(0, \pi)$ . Here we will take  $\mu = 2.0$  which corresponds to having 2.32 electron persite and gives the Fermi surface shown in Fig. 1 (a). There are four Fermi pockets in the Brillouin zone:  $\alpha_1$  around  $(0, 0)$  and  $\alpha_2$  around  $(\pi, \pi)$  are hole pockets associated with  $E_{-}(\mathbf{k}_f) = 0$ , while  $\beta_1$  around  $(\pi, 0)$  and  $\beta_2$  around  $(0, \pi)$  are electron pockets given by  $E_{+}(\mathbf{k}_f) = 0$ . For this minimal model, we will include only onsite intra and inter orbital Coulomb interactions, which will both be set equal to  $U$  and we will neglect the Hunds rule coupling. In this case, up to a shift of the chemical potential, the interaction can be written as

$$\hat{H}_{int} = \frac{U}{2} \sum_i \left( \sum_{\sigma} \psi_{\sigma}^{\dagger}(i) \mathbf{1} \psi_{\sigma}(i) \right)^2 \quad (5)$$

An important feature of this two band model is the nontrivial  $C_4$  rotation symmetry of the two orbitals. Under a  $90^\circ$  degree rotation, the two orbitals transform as  $|xz\rangle \rightarrow |yz\rangle$  and  $|yz\rangle \rightarrow -|xz\rangle$ . Correspondingly, in the Hamiltonian,  $\epsilon_{+}(\mathbf{k})$  has  $s$ -wave symmetry and  $\epsilon_{-}(\mathbf{k})$  and  $\epsilon_{xy}(\mathbf{k})$  have  $d$ -wave symmetry, which together preserve the point group symmetry of the Hamiltonian. Consequently, the wave functions  $a_{\nu,\mathbf{k}}^s$  of the energy eigenstates also have nontrivial structure in the Brillouin zone,

which can be determined by the direction of the vector  $\mathbf{n}(\mathbf{k}) = (\epsilon_{-}(\mathbf{k}), \epsilon_{xy}(\mathbf{k}))$ . If we consider the orbital degree of freedom as a pseudo-spin, the electrons in the lower band always have a “pseudo-spin” anti-parallel to  $\mathbf{n}(\mathbf{k})$ . For the parameters we are using, the distribution of the unit vector  $\hat{\mathbf{n}}(\mathbf{k}) = \mathbf{n}(\mathbf{k})/|\mathbf{n}(\mathbf{k})|$  is shown in Fig. 1 (b). For example, at the wavevector  $\mathbf{k} = (\pi/2, 0)$  we have  $\epsilon_{-}(\mathbf{k}) < 0$  and  $\epsilon_{xy}(\mathbf{k}) = 0$ , which means the upper band is formed from  $xz$  orbitals and the lower band from  $yz$  orbitals. From Fig. 1 (b) we can see that the electron pocket  $\beta_1$  ( $\beta_2$ ) is formed mainly from  $xz$  ( $yz$ ) orbitals, while the hole pockets are formed from “ $d$ -wave” superposition of the two orbitals. This point will be important for understanding the pairing symmetry. Since this non-trivial structure of the wave function originates from the symmetry of the two orbitals  $d_{xz}$  and  $d_{yz}$ , we expect it to be qualitatively correct even beyond the present two orbital model.

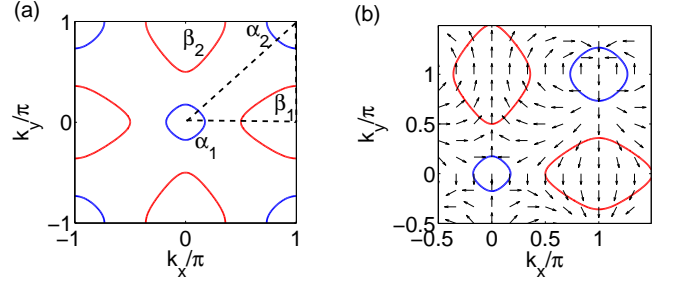


FIG. 1: (a) The Fermi surface of the 2-orbital model on the large 1Fe/cell BZ. Here, the  $\alpha_{1,2}$  surfaces are hole Fermi pockets given by  $E_{-}(\mathbf{k}_f) = 0$  and the  $\beta_{1,2}$  surfaces are electron Fermi pockets given by  $E_{+}(\mathbf{k}_f) = 0$ . In this paper we have set  $t_1 = -1, t_2 = 1.3, t_3 = t_4 = -0.85$  and  $\mu = 2$ . (b) Wave function distribution in the Brillouin zone. The arrows show the direction of the vector  $(\epsilon_{-}(\mathbf{k}), \epsilon_{xy}(\mathbf{k}))$ . When an arrow is pointing up (down) at some  $\mathbf{k}$  point, the eigenstate of upper band  $E_{+}(\mathbf{k})$  consists of pure  $xz$  ( $yz$ ) orbitals. The Brillouin zone is shifted by  $(\pi/2, \pi/2)$  for convenience.

In the following we first discuss the particle-hole susceptibility and calculate it using an RPA approximation. Then using the pairing interaction associated with the exchange of these particle-hole excitations, we examine the strength of the pairing in the singlet and triplet channels.

*One loop and RPA susceptibilities* - Because of the two-orbitals, the generic form of the susceptibility depends on four orbital indices  $p, q, s, t$  equal to 1 or 2 for  $d_{xz}$  and  $d_{yz}$ , as well as spin indices:

$$\begin{aligned} \chi_{s\alpha,t\beta}^{p\gamma,q\delta}(\mathbf{q}, i\Omega) &= \int \frac{d^2\mathbf{k}}{(2\pi)^2} \int_0^\beta d\tau e^{i\Omega\tau} \langle T_\tau \psi_{t\beta,\mathbf{k}-\mathbf{q}}^{\dagger}(\tau) \\ &\quad \cdot \psi_{s\alpha,\mathbf{k}}(\tau) \psi_{p\gamma,\mathbf{k}'+\mathbf{q}}^{\dagger}(0) \psi_{q\delta,\mathbf{k}'}(0) \rangle \end{aligned} \quad (6)$$

Due to the  $SU(2)$  spin rotation symmetry, the suscepti-

bility function has the following form:

$$\chi_{s\alpha,t\beta}^{pq,\gamma\delta}(\mathbf{q}, i\Omega) = \frac{1}{6}\chi_{1st}^{pq}\vec{\sigma}_{\beta\alpha} \cdot \vec{\sigma}_{\gamma\delta} + \frac{1}{2}\chi_{0st}^{pq}\delta_{\beta\alpha}\delta_{\gamma\delta} \quad (7)$$

where  $\chi_1$  and  $\chi_0$  correspond to the correlation functions of the triplet fields (such as spin) and the singlet fields (such as charge density), respectively. All the physical susceptibilities are determined by some components of  $\chi_{0,1st}^{pq}$ . For example, the total spin susceptibility is given by  $\chi_S = \frac{1}{2}\sum_{s,p}\chi_{1ss}^{pp}$ . At the one-loop level, we have  $\chi_{0st}^{pq}(\mathbf{q}, i\Omega) = \chi_{1st}^{pq}(\mathbf{q}, i\Omega)$ , which we denote by  $\chi_{st}^{pq}(\mathbf{q}, i\Omega)$ . For a given  $(\mathbf{q}, i\Omega)$ ,  $\chi_{0st}^{pq}$  and  $\chi_{1st}^{pq}$  are  $4 \times 4$  matrices, and the RPA susceptibility is obtained from the matrix equation

$$\chi_{0(1)}^{\text{RPA}}(\mathbf{q}, i\Omega) = \chi(\mathbf{q}, i\Omega) (\mathbb{I} - \gamma_{0(1)}\chi(\mathbf{q}, i\Omega))^{-1} \quad (8)$$

with

$$\gamma_1 = U\mathbb{I}_{4 \times 4}, \quad \gamma_0 = \begin{pmatrix} -U & & & \\ & U & & \\ & & U & \\ & & & -U \end{pmatrix}, \quad (9)$$

in the basis  $(st) = (11, 21, 12, 22)$ . The one-loop susceptibility  $\chi_{st}^{pq}(\mathbf{q}, i\Omega)$  is given by

$$\chi_{st}^{pq}(\mathbf{q}; i\Omega) = - \int \frac{d^2\mathbf{k}}{(2\pi)^2} \frac{a_{\nu,\mathbf{k}+\mathbf{q}}^{t*} a_{\nu',\mathbf{k}}^s a_{\nu',\mathbf{k}}^{p*} a_{\nu,\mathbf{k}+\mathbf{q}}^q}{i\Omega + E_{\nu,\mathbf{k}+\mathbf{q}} - E_{\nu',\mathbf{k}}} \cdot (n_F(E_{\nu,\mathbf{k}+\mathbf{q}}) - n_F(E_{\nu',\mathbf{k}})) \quad (10)$$

with  $a_{\nu,\mathbf{k}}^s$  defined by Eq. (3).

In Fig. 2 (a), the one loop spin susceptibility  $\chi_S(\mathbf{q}, \omega = 0)$  versus momentum  $\mathbf{q}$  for  $\mu = 2.0$  is shown as the solid curve. The dashed curve shows the maximal eigenvalue of the one-loop susceptibility matrix  $\chi_{st}^{pq}$  along the same contour. From this, we see that there is a critical value  $U_c \simeq 3$ , at which the  $S = 1$  generalized RPA susceptibility diverges at an incommensurate wave vector near  $\mathbf{q} \simeq (\pi/2, \pi/2)$ . This divergence occurs in the spin-one part of the particle-hole channel and reflects a superposition of particle-hole spin-one fluctuations involving both orbitals. The RPA spin susceptibility for  $U = 2.8$  is also shown in Fig. 2 (b), which, as expected, shows the strongest enhancement near  $\mathbf{q} = (\pi/2, \pi/2)$ .

*Superconductivity* - Within an RPA approximation, the singlet and triplet pairing vertices are given by[25]

$$\begin{aligned} \Gamma_{0st}^{pq}(\mathbf{k}, \mathbf{k}', i\Omega) &= -\frac{1}{2}(U_0 - 3U_1)_{ps}^{tq}(\mathbf{k} - \mathbf{k}', i\Omega) \\ \Gamma_{1st}^{pq}(\mathbf{k}, \mathbf{k}', i\Omega) &= -\frac{1}{2}(U_0 + U_1)_{ps}^{tq}(\mathbf{k} - \mathbf{k}', i\Omega) \end{aligned} \quad (11)$$

Here  $U_{0ps}^{tq} = [\frac{1}{2}\gamma_0 + \gamma_0\chi_0^{\text{RPA}}\gamma_0]_{ps}^{tq}$  and  $U_{1ps}^{tq} = [\frac{1}{2}\gamma_1 + \gamma_1\chi_1^{\text{RPA}}\gamma_1]_{ps}^{tq}$  describe the effective interaction mediated by orbital and spin fluctuation respectively. It

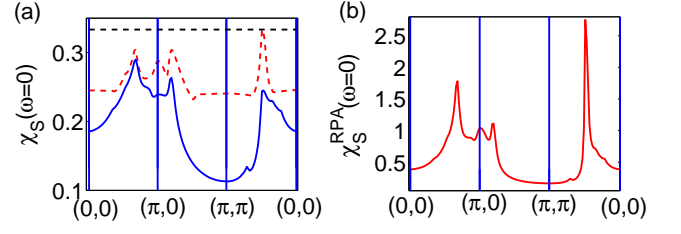


FIG. 2: (a) The static one loop spin susceptibility (solid line) and the largest eigenvalue of one loop susceptibility matrix  $\chi_{st}^{pq}$  along the  $(0,0) \rightarrow (\pi,0) \rightarrow (\pi,\pi) \rightarrow (0,0)$  contour in the Brillouin zone. The horizontal dashed line shows the value of  $1/U_c = 1/3$  which indicates the critical  $U_c = 3$ . (b) The RPA spin susceptibility for  $U = 2.8$ .

should be noticed that the order of orbital indices is different for  $U_{0,1}$  and  $\Gamma_{0,1}$ .

Just as for the traditional phonon case, retardation is important and what enters in characterizing the strength of the pairing interaction is

$$\int_0^\infty \frac{d\omega}{\pi} \frac{\text{Im} [\Gamma_{0(1)st}^{pq}(\mathbf{k}, \mathbf{k}', \omega)]}{\omega} = \text{Re} [\Gamma_{0(1)st}^{pq}(\mathbf{k}, \mathbf{k}', \omega = 0)] \quad (12)$$

in which a Wick rotation  $i\Omega \rightarrow \omega + i\delta$  has been performed on  $\Gamma_{0,1}(\mathbf{k}, \mathbf{k}', i\Omega)$ . The interaction induces scattering of two Cooper pairs around the Fermi surfaces. For later convenience, we define  $C_i, i = 1, \dots, 4$  as the four pieces of Fermi pockets  $\alpha_1, \alpha_2, \beta_1, \beta_2$ , and  $\gamma_{i\sigma\mathbf{k}}$  the annihilation operator of the electron around the  $i^{\text{th}}$  Fermi surface pocket with wavevector  $\mathbf{k} \in C_i$ . Thus  $\gamma_{i\sigma\mathbf{k}}$  is equal to  $\gamma_{\nu_i, \sigma\mathbf{k}}$  defined in Eq. (2) with  $\nu_i = +1(-1)$  when  $C_i$  is an electron (hole) pocket. The Cooper pair defined here can be either a singlet or a triplet. Here and below we omit the spin indices since the spin state is determined by the parity of the gap when  $\mathbf{k}$  goes to  $-\mathbf{k}$ . The scattering of a Cooper pair from  $(\mathbf{k}, -\mathbf{k})$  on the  $i^{\text{th}}$  Fermi surface to  $(\mathbf{k}', -\mathbf{k}')$  on the  $j^{\text{th}}$  Fermi surface is determined by the projection of the interaction vertex  $\Gamma_{0,1st}^{pq}(\mathbf{k}, \mathbf{k}')$  to the energy eigenstates:

$$\Gamma_{0,1ij}(\mathbf{k}, \mathbf{k}') = \sum_{s,t,p,q} a_{\nu_i, -\mathbf{k}}^{t*} a_{\nu_i, \mathbf{k}}^{s*} \Gamma_{0,1st}^{pq}(\mathbf{k}, \mathbf{k}') a_{\nu_j, \mathbf{k}}^p a_{\nu_j, -\mathbf{k}'}^q \quad (13)$$

with  $\mathbf{k} \in C_i, \mathbf{k}' \in C_j$ .

For a pairing configuration mediated by  $\Delta(\mathbf{k}) = g(\mathbf{k})\gamma_{i,-\mathbf{k}}\gamma_{i,\mathbf{k}}, \mathbf{k} \in C_i$ , a dimensionless *coupling strength functional* is defined as[26]

$$\lambda[g(\mathbf{k})] = - \frac{\sum_{i,j} \oint_{C_i} \frac{d\mathbf{k}_{\parallel}}{v(\mathbf{k})} \oint_{C_j} \frac{d\mathbf{k}'_{\parallel}}{v(\mathbf{k}')} g(\mathbf{k}) \Gamma_{ij}^{[g]}(\mathbf{k}, \mathbf{k}') g(\mathbf{k}')}{(2\pi)^2 \sum_i \oint_{C_i} \frac{d\mathbf{k}_{\parallel}}{v(\mathbf{k})} g^2(\mathbf{k})} \quad (14)$$

in which  $v(\mathbf{k}) = |\nabla_{\mathbf{k}} E_{\nu(i)}(\mathbf{k})|$  for  $\mathbf{k} \in C_i$  is the fermi velocity, and  $\oint_{C_i} \frac{d\mathbf{k}_{\parallel}}{v(\mathbf{k})}$  is a loop integral around the  $C_i$  fermi surfaces.  $\Gamma_{ij}^{[g]}(\mathbf{k}, \mathbf{k}') = \Gamma_{0(1)ij}(\mathbf{k}, \mathbf{k}')$  when  $g(\mathbf{k})$  has

even (odd) parity, respectively. For a given  $\Gamma_{0,1ij}(\mathbf{k}, \mathbf{k}')$ , the optimum pairing configuration and corresponding  $\lambda$  can be determined by solving an eigenvalue problem

$$-\sum_j \oint_{C_j} \frac{d\mathbf{k}'_{\parallel}}{(2\pi)^2 v(\mathbf{k}')} \Gamma_{ij}^{[g]}(\mathbf{k}, \mathbf{k}') g(\mathbf{k}') = \lambda g(\mathbf{k}), \quad (15)$$

which is obtained from the stationary condition  $\delta\lambda[g(\mathbf{k})]/\delta g(\mathbf{k}) = 0$ .

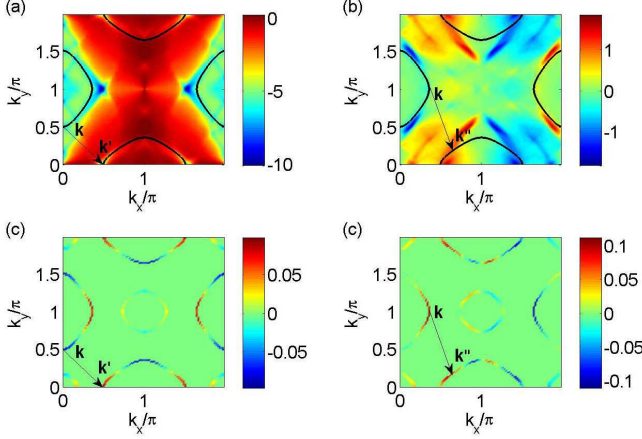


FIG. 3: (a) The effective interaction  $\Gamma_{0++}(\mathbf{k}, \mathbf{k}')$  describing the scattering of singlet Cooper pairs on and between electron pockets. One wavevector  $\mathbf{k}$  is fixed and the color shows the value of  $\Gamma_{0++}(\mathbf{k}, \mathbf{k}')$  as a function of  $\mathbf{k}'$ . (b) The same plot as (a) for the triplet channel  $\Gamma_{1++}(\mathbf{k}, \mathbf{k}')$ . (c) and (d) shows the optimum singlet and triplet pairing configurations. The arrow in each figure indicates a typical inter Fermi surface scattering process.

The interaction  $\Gamma_{0,1ij}(\mathbf{k}, \mathbf{k}')$  contains various intra Fermi surface and inter Fermi surface scattering processes. However, for  $\mu = 2.0$  we find that scattering on and between the  $\beta_1$  and  $\beta_2$  electron pockets is dominant. From the definition (13) we see that  $\Gamma_{0,1ij}$  only depends on the band label  $\nu_i, \nu_j$ . Thus the scattering on and between the two electron pockets are determined by  $\Gamma_{0,1++}(\mathbf{k}, \mathbf{k}')$  Eq. (13), since  $\nu_i = \nu_j = +1$  (which we have shortened to  $+$ ). The distribution of the effective singlet  $\Gamma_{0++}(k, k')$  and triplet  $\Gamma_{1++}(k, k')$  interactions for  $U = 2.8$  are shown in Fig. 3 (a) and (b) respectively for a fixed  $\mathbf{k} \in \beta_2$ . From the figure it can be seen that the interaction for singlet pairing is repulsive, which favors a pairing configuration with a node. The interaction in the triplet channel has a smaller magnitude than the singlet, but is still sizable and can support a p-wave triplet state. The relative sign of the order parameter on the two fermi pockets is determined by the inter Fermi surface scattering. For example,  $\Gamma_{0++}(\mathbf{k}, \mathbf{k}')$  is repulsive for the choice of  $\mathbf{k}$  and  $\mathbf{k}'$  shown by the arrow in Fig. 3 (a) and (c), so that the pairing amplitude has opposite signs at  $\mathbf{k}$  and  $\mathbf{k}'$ . For a similar reason the pairing amplitude in Fig. 3 (b) and (d) has the same sign at  $\mathbf{k}$  and  $\mathbf{k}''$ .

By solving Eq. (15), we obtain the optimum singlet and triplet pairing configurations shown in Fig. 3 (c) and (d) respectively. We find that  $\lambda_0 = 0.46$  for singlet pairing and  $\lambda_1 = 0.20$  for triplet pairing. To see the contributions of intra Fermi surface and inter Fermi surface scattering processes, we calculate these two terms separately by defining  $\lambda_{ij}$  as the term in Eq. (14) that involves the scattering from the  $i$  to the  $j$  Fermi surface. The total  $\lambda$  is given by  $\lambda = \sum_{i,j} \lambda_{ij}$ . For  $i, j = \beta_1, \beta_2$ ,  $\lambda_{0,1ij}$  are  $2 \times 2$  matrices, which for  $U = V = 2.8$  are

$$\lambda_0 = \begin{pmatrix} 0.15 & 0.083 \\ 0.083 & 0.15 \end{pmatrix}, \quad \lambda_1 = \begin{pmatrix} -0.026 & 0.10 \\ 0.10 & 0.025 \end{pmatrix} \quad (16)$$

Here one sees that the inter Fermi surface scattering makes an important contribution to the pairing strength  $\lambda$ . It should be noticed that the singlet pairing configuration has the same diagonal term  $\lambda_{ii}$  for  $i = \beta_1$  and  $\beta_2$  while the p-wave diagonal terms  $\lambda_{ii}$  can have different values.

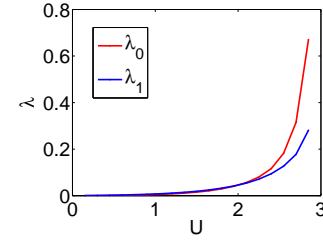


FIG. 4: The singlet  $\lambda_0$  and triplet  $\lambda_1$  pairing strength as a function of  $U$ .

We have also studied the dependence of the pairing strength upon the interaction  $U$ . As shown in Fig. 4, the strength of both the singlet d-wave and triplet p-wave pairing channels is increased as  $U$  increases. Within the RPA approximation, the coupling strength formally diverges as  $U$  approaches the critical point  $U_c \approx 3.0$  associated with the onset of order in the spin one particle-hole channel. This is similar to the behavior found for the  $d_{x^2-y^2}$  coupling in the two-dimensional Hubbard model when an RPA approximation is used to treat the pairing due to the exchange coupling of spin-fluctuations. Just as for that case, one needs to go beyond the RPA to determine the actual behavior of the model.

In order to gain further insight into the nature of the pairing, it is useful to determine the real space pairing structure which corresponds to  $\Delta(\mathbf{k})$  shown in Fig. 3 (c) and (d). This can be obtained from  $\Delta^\dagger = \sum_{\mathbf{k}} g(\mathbf{k}) \gamma_{+\uparrow}^\dagger(\mathbf{k}) \gamma_{+\downarrow}^\dagger(-\mathbf{k})$  by transforming the band operator to orbital operators, Eq (3), and Fourier transforming to the lattice coordinates. As discussed earlier, the states associated with the two electron pockets  $\beta_1$  and  $\beta_2$  are formed primarily from  $xz$  and  $yz$  orbitals, respectively, as shown in Fig. 1 (b). With this in mind, we find that the singlet pairing in Fig 5(c) corresponds to a superposition of singlets formed from electrons in near-neighbor

$d_{xz}$  orbitals minus a similar super position involving the  $d_{yz}$  orbitals.

$$\Delta_d^\dagger = \frac{1}{N} \sum_{r, \hat{\delta}=\hat{x}, \hat{y}} (\psi_{x\uparrow}^\dagger(r) \psi_{x\downarrow}^\dagger(r + \hat{\delta}) - \psi_{x\downarrow}^\dagger(r) \psi_{x\uparrow}^\dagger(r + \hat{\delta})) - (\psi_{y\uparrow}^\dagger(r) \psi_{y\downarrow}^\dagger(r + \hat{\delta}) - \psi_{y\downarrow}^\dagger(r) \psi_{y\uparrow}^\dagger(r + \hat{\delta})) \quad (17)$$

Under a 90 degree rotation  $\psi_{x\sigma}^\dagger \rightarrow \psi_{y\sigma}^\dagger$  and  $\psi_{y\sigma}^\dagger \rightarrow -\psi_{x\sigma}^\dagger$ , so that  $\Delta_d^\dagger$  changes sign, corresponding to a d-wave gap. For the p-wave triplet shown in Fig 5(d), we find that

$$\Delta_p^\dagger = \frac{1}{N} \sum_{r, \hat{\delta}=\hat{x}, \hat{y}} (\psi_{x\uparrow}^\dagger(r) \psi_{x\uparrow}^\dagger(r + \hat{\delta}) + \psi_{y\uparrow}^\dagger(r) \psi_{y\uparrow}^\dagger(r + \hat{\delta})) \quad (18)$$

Note that this triplet gap is associated with a near neighbor intra-orbital pairing rather than the onsite inter-orbital triplet pairing proposed in Ref. 21.

*Conclusion* - We have studied the pairing interaction associated with the exchange of particle-hole fluctuation for a two-orbital  $d_{xz}$ - $d_{yz}$  Hubbard model. By adjusting the tight binding parameters, one can obtain Fermi surface with hole and electron pockets which are similar to those found in bandstructure calculations for LaOFeAs. For a filling of two electrons per site, the signs of the hole and electron pockets are similar and the RPA spin susceptibility becomes singular as the on site intra and inter Coulomb interaction  $U$  increase. This SDW singularity occurs at a wave vector  $q = (\pi, 0)$  and  $(0, \pi)$  associated with the nesting of the hole and electron pockets. When this model is doped, the hole pockets shrink and the electron pockets become dominant. In this case, the SDW  $q = (\pi, 0)$  singularity in the spin susceptibility is suppressed and there is a strong response in the spin one particle-hole channel near  $q \approx (\pi/2, \pi/2)$ . The pairing interaction associated with the exchange of these fluctuation leads to an attractive interaction for both singlet d-wave and triplet p-wave pairing, which compete closely. The singlet d-wave pairing strength grows faster than the triplet p-wave pairing strength as the interactions are increased and a magnetic instability is approached. However, more refined numerical calculations beyond the RPA approximation are needed to uniquely select among the two competing pairing states.

*Acknowledgement* - We acknowledge helpful discussions with X. Dai, Z. Fang, S. Kivelson, T. Maier, R. Martin, I. Mazin, T. Schulthess, D. Singh and H. Yao. This work is supported by the NSF under grant numbers DMR-0342832, the US Department of Energy, Office of Basic Energy Sciences under contract DE-AC03-76SF00515, the center for nanophase material science, ORNL (DJS) and the Stanford Institute for Theoretical Physics (SR, DJS).

*Note added* - After completing this work, we learned that a similar work has been done by Z.-J. Yao, J.-X. Li and Z. D. Wang, which is posted in arXiv:0804.4116[27].

- 
- [1] Y. Kamihara, T. Watanabe, M. Hirano, and H. Hosono, J. Am. Chem. Soc. **130**, 3296 (2008).
  - [2] Z.-A. Ren, J. Yang, W. Lu, G.-C. Che, X.-L. Dong, L.-L. Sun, and Z.-X. Zhao, e-print arxiv: 0803.4283 (2008).
  - [3] G. Chen, Z. Li, G. Li, J. Zhou, D. Wu, W. Hu, P. Zheng, Z. Chen, J. Luo, and N. Wang, e-print arxiv: 0803.0128 (2008).
  - [4] X. Chen, T. Wu, G. Wu, R. Liu, H. Chen, and D. Fang, e-print arxiv: 0803.3603 (2008).
  - [5] G. Chen, Z. Li, D. Wu, G. Li, W. Z. Hu, J. Dong, P. Zheng, J. Luo, and N. Wang, e-print arxiv: 0803.3790 (2008).
  - [6] H.-H. Wen, G. Mu, L. Fang, H. Yang, and X. Zhu, Europhys. Lett. **82**, 17009 (2008).
  - [7] Z.-A. Ren, W. Lu, J. Yang, W. Yi, X.-L. Shen, Z.-C. Li, G.-C. Che, X.-L. Dong, L.-L. Sun, F. Zhou, et al., e-print arxiv: 0804.2053 (2008).
  - [8] Z.-A. Ren, G.-C. Che, X.-L. Dong, J. Yang, W. Lu, W. Yi, X.-L. Shen, Z.-C. Li, L.-L. Sun, F. Zhou, et al., e-print arxiv: 0804.2582 (2008).
  - [9] B. Lorenz, K. Sasmal, R. P. Chaudhury, X. H. Chen, R. H. Liu, T. Wu, and C. W. Chu, e-print arxiv: 0804.1582 (2008).
  - [10] G. Mu, X. Zhu, L. Fang, L. Shan, C. Ren, and H.-H. Wen, e-print arxiv: 0803.0928 (2008).
  - [11] L. Ding, C. He, J. Dong, T. Wu, R. Liu, X. Chen, and S. Li, e-print arxiv: 0804.3642 (2008).
  - [12] L. Shan, Y. Wang, X. Zhu, G. Mu, L. Fang, and H.-H. Wen, e-print arxiv: 0803.2405 (2008).
  - [13] F. Hunte, J. Jaroszynski, A. Gurevich, D. Larbalestier, R. Jin, A. Sefat, M. McGuire, B. Sales, D. Christen, and D. Mandrus, e-print arxiv: 0804.0485 (2008).
  - [14] X. Zhu, H. Yang, L. Fang, G. Mu, and H.-H. Wen, e-print arxiv: 0803.1288 (2008).
  - [15] K. Ahilan, F. Ning, T. Imai, A. Sefat, R. Jin, M. McGuire, B. Sales, and D. Mandrus, e-print arxiv: 0804.4026 (2008).
  - [16] J. Dong, H. J. Zhang, G. Xu, Z. Li, G. Li, W. Z. Hu, D. Wu, G. F. Chen, X. Dai, J. L. Luo, et al., e-print arxiv:0803.3426 (2008).
  - [17] C. de la Cruz, Q. Huang, J. W. Lynn, J. Li, W. R. II, J. L. Zarestky, H. A. Mook, G. F. Chen, J. L. Luo, N. L. Wang, et al., e-print arxiv: 0804.0795 (2008).
  - [18] H.-J. Zhang, G. Xu, X. Dai, and Z. Fang, e-print arxiv: 0803.4487 (2008).
  - [19] G. Xu, W. Ming, Y. Yao, X. Dai, S.-C. Zhang, and Z. Fang, e-print arxiv: 0803.1282 (2008).
  - [20] X. Dai, Z. Fang, Y. Zhou, and F.-C. Zhang, e-print arxiv: 0803.3982 (2008).
  - [21] P. A. Lee and X.-G. Wen, e-print arxiv: 0804.1739 (2008).
  - [22] I. Mazin, D. Singh, M. Johannes, and M.-H. Dou, e-print arxiv: 0803.2740 (2008).
  - [23] S. Raghu, X.-L. Qi, C.-X. Liu, D. Scalapino, and S.-C. Zhang, e-print arxiv:0804.1113 (2008).
  - [24] D. Singh and M.-H. Du, e-print arxiv: 0803.0429 (2008).
  - [25] T. Takimoto, T. Hotta, and K. Ueda, Phys. Rev. B **69**, 104504 (2004).
  - [26] D. Scalapino, E. Loh, and J. Hirsch, Phys. Rev. B **34**, 8190 (1986).
  - [27] Z.-J. Yao, J.-X. Li, and Z. D. Wang, e-print arxiv:

0804.4166 (2008).